HHS Public Access

Author manuscript

Nat Med. Author manuscript; available in PMC 2013 July 26.

Published in final edited form as:

Nat Med. 2012 August ; 18(8): 1232–1238. doi:10.1038/nm.2827.

Neural precursor cells induce cell death of high-grade astrocytomas via stimulation of TRPV1

Kristin Stock[1,*], **Jitender Kumar**[1,*], **Michael Synowitz**[1,2,*], **Stefania Petrosino**[3], **Roberta Imperatore**[4], **Ewan St. J. Smith**[5,6], **Peter Wend**[7], **Bettina Purfürst**[8], **Ulrike A. Nuber**[9], **Ulf Gurok**[10], **Vitali Matyash**[1], **Joo-Hee Wälzlein**[1], **Sridhar R. Chirasani**[1], **Gunnar Dittmar**[11], **Benjamin F. Cravatt**[12], **Stefan Momma**[13], **Gary R. Lewin**[5], **Alessia Ligresti**[3], **Luciano De Petrocellis**[4], **Luigia Cristino**[4], **Vincenzo Di Marzo**[3], **Helmut Kettenmann**[1,*], and **Rainer Glass**[1,14,*]

[1]Cellular Neuroscience, Max Delbrück Centre for Molecular Medicine (MDC), 13125 Berlin, Germany

[2]Department of Neurosurgery, Charité - University Medicine Berlin, 13353 Berlin, Germany

[3]Endocannabinoid Research Group, Institute of Biomolecular Chemistry, Consiglio Nazionale delle Ricerche, 80078 Pozzuoli (NA), Italy

[4]Endocannabinoid Research Group, Institute of Cybernetics, Consiglio Nazionale delle Ricerche, 80078 Pozzuoli (NA), Italy

[5]Molecular Physiology of Somatic Sensation, Max Delbrück Centre for Molecular Medicine (MDC), 13125 Berlin, Germany

[6]Skirball Institute of Biomolecular Medicine, New York University Langone Medical Center, New York NY 10016

[7]Signal Transduction, Epithelial Differentiation, Invasion and Metastasis (Present address: David Geffen School of Medicine and Jonsson Comprehensive Cancer Center, University of California at Los Angeles, CA 90095, USA), Max Delbrück Centre for Molecular Medicine (MDC), 13125 Berlin, Germany

[8]Central Facility for Electron Microscopy, Max Delbrück Centre for Molecular Medicine (MDC), 13125 Berlin, Germany

[9]Lund Center for Stem Cell Biology and Cell Therapy, Lund University, SE-221 00 Lund, Sweden

Correspondence: Rainer Glass; Neurosurgical Research, Department of Neurosurgery, Ludwig Maximilians University (LMU), Marchioninistr 15, D-81377 Munich Tel: +49 89 70953148; rainer.glass@med.uni-muenchen.de.

*These authors contributed equally.

Accession numbers:
GSE37671

Author contributions:

SP, RI, AL, LDP, UG and SRC designed the experiments, conducted the experiments and interpreted the data; KS, JK, EStJS, PW, BP, UAN, VDM, JHW, GD and LC additionally contributed to manuscript preparation. GRL, VDM and HK designed the experiments, supervised the project, interpreted the data and contributed to manuscript preparation. MS performed brain tumor resections and provided tumor samples. MS and RG designed the experiments, conducted the experiments, supervised the project, interpreted the data and prepared the manuscript.

[10]Max Planck Institute for Molecular Genetics, 14195 Berlin, Germany

[11]Central Facility for Mass Spectrometry, Max Delbrück Centre for Molecular Medicine (MDC), 13125 Berlin, Germany

[12]The Scripps Research Institute, SR107, 10550 North Torrey Pines Road, La Jolla, CA 92037

[13]Restorative Neurology, Institute of Neurology (Edinger-Institute), Johann Wolfgang Goethe-University Frankfurt, 60528 Frankfurt am Main, Germany

[14]Neurosurgical Research, Department of Neurosurgery, Ludwig Maximilians University of Munich, 81377 Munich, Germany

Abstract

Primary astrocytomas of World Health Organization grade 3 and grade 4 (HG-astrocytomas) are preponderant among adults and are almost invariably fatal despite multimodal therapy. Here, we show that the juvenile brain has an endogenous defense mechanism against HG-astrocytomas. Neural precursor cells (NPCs) migrate to HG-astrocytomas, reduce glioma expansion and prolong survival by releasing a group of fatty acid ethanolamides that have agonistic activity on the vanilloid receptor (transient receptor potential vanilloid subfamily member-1; TRPV1). TRPV1 expression is higher in HG-astrocytomas than in tumor-free brain and TRPV1 stimulation triggers tumor cell death via the activating transcription factor-3 (ATF3) controlled branch of the ER stress pathway. The anti-tumorigenic response of NPCs is lost with aging. NPC-mediated tumor suppression can be mimicked in the adult brain by systemic administration of the synthetic vanilloid Arvanil, suggesting that TRPV1 agonists hold potential as new HG-astrocytoma therapeutics.

Introduction

Somatic mutant neural stem and precursor cells (NPCs) are thought to be the source for high-grade astrocytomas (HG-astrocytomas), one of the most aggressive forms of CNS tumors[1]. HG-astrocytomas and glioblastomas (GBM) are much more frequent in adults than in children[2,3]. However, adult neurogenesis, that is the presence and activity of NPCs in the postnatal and adult brain, is maintained at high rate only until puberty and declines thereafter[4,5]. Hence, the epidemiology of glioblastomas and the timing of adult neurogenesis are inversely correlated and glioblastomas are usually diagnosed several decades after the decline in brain stem cell activity.

It has been previously found that endogenous and exogenous NPCs have a strong tropism for primary brain tumors and that NPCs can release tumor-suppressive factors[6–13]. However, the molecular nature of the factors that mediate cell death in HG-astrocytoma cells has not been identified. We show that HG-astrocytoma associated NPCs induce tumor cell death via the release of endovanilloids. Endovanilloids[14] like arachidonoyl-ethanolamide (AEA) and N-arachidonoyl-dopamine (NADA) directly stimulate the vanilloid receptor (TRPV1; transient receptor potential vanilloid-1)[15]. Synergistic TRPV1 activation by AEA in combination with other fatty acid ethanolamides such as oleoyl-ethanolamide (OEA) or palmitoyl-ethanolamide (PEA) is also observed[15,16]. TRPV1 is a non-selective

cation channel that is best characterized in capsaicin-sensitive sensory neurons of the dorsal root and trigeminal ganglia[16]. The physiological role of the ion channel in non-neural tissues is largely unexplored[16].

Results

NPCs induce HG-astrocytoma cell death via TRPV1

We investigated the signaling pathways that are activated in HG-astrocytoma cells after exposure to NPC conditioned medium (NPC-CM). Analysis of gene expression changes together with pharmacological and molecular studies (for microarray data, please refer to Gene expression omnibus repository; GSE37671) suggested a role for NPC-derived endovanilloids as tumor suppressors. Furthermore, we observed that TRPV1 expression positively correlates with grading in human primary brain tumors whereas little TRPV1 is detected in human tumor-free brain tissue; data from real-time PCR (Supplementary Fig. 1a) were supported by immunohistochemistry on tissue panels (not shown).

Next, we explored the role of the endovanilloid system in NPC-mediated HG-astrocytoma suppression in an established mouse model[8,9,17]. Here, we induced orthotopic brain tumors in Nestin-GFP mice, which are a model for the visualization of NPCs[8,18] (Fig. 1a). Subventricular NPCs migrated to HG-astrocytomas that were located in the caudate putamen[8,9,17]. NPCs were identified by co-localization of GFP with established immunocytochemical markers such as PSA-Ncam (Fig. 1b) or Musashi[8,19,20]. PSA-NCAM is also a marker for tumor-associated NPCs in humans (S. Momma, personal communication). Importantly, we found that mouse HG-astrocytomas express high levels of TRPV1 (Fig. 1c); i.e. TRPV1 levels in tumors were higher than in tumor-free brain, while only a small fraction of tumor associated Nestin-GFP$^+$ cells expressed TRPV1; TRPV1 was absent from subventricular NPCs (Supplementary Fig. 1b).

In a series of *in vitro* experiments, we found that factors released from mouse NPCs (mNPC-CM), but not from their fully differentiated progeny (i.e. astrocytes, oligodendrocytes and neurons) or from fibroblasts (scrc), strongly reduced the viability of mouse HG-astrocytoma cells over a time-course of three days (Fig. 1d). In subsequent experiments HG-astrocytoma cells were always stimulated for three days, unless indicated otherwise. mNPC-CM reduced tumor cell viability by inducing cell death, as indicated by TUNEL- and cytotoxicity-assays (Supplementary Fig. 1c). Cytotoxicity values are given as percent of fully permeabilized cells (raw data are presented in Supplementary Fig. 2 and 3).

GL261 HG-astrocytomas express TRPV1 and contain specific binding sites for a selective TRPV1 ligand (Supplementary Fig. 1d,e). Importantly, mNPC-CM induced HG-astrocytoma cell death was greatly reduced by blocking TRPV1 with the selective antagonists[16] iodo-resiniferatoxin (I-RTX, 10 nM; Fig. 1e) or capsazepine (CZP, 1 μM; Fig. 1e) and by TRPV1-knock down (TRPV1-KD; Fig. 1e). We verified TRPV1-KD efficiency (Supplementary Fig. 1d,e) and specificity by performing experiments with control shRNAs (scrambled) and over-expression of a knock-down resistant form of mouse-TRPV1[21] in TRPV1-KD tumor cells (rescue; Fig. 1e and 2f;, Supplementary Fig. 2c). mNPC-CM strongly induced cell death in different HG-astrocytoma cell lines (Fig. 1f) and a range of

primary human glioblastomas (Fig. 1g), an effect that was always blocked by co-application of either I-RTX (Supplementary Fig. 2b, 3a and 3b) or CZP. Importantly, conditioned medium from human NPCs (human NPC-CM) also induced cell death in primary human glioblastomas after TRPV1 stimulation (Fig. 1h).

Overall, we observed that TRPV1 levels in HG-astrocytomas are much higher than in normal brain. NPCs migrate to brain tumors *in vivo. In vitro* experiments showed that human and mouse NPCs release endovanilloids (TRPV1 agonists) which induce HG-astrocytoma cell death.

NPCs constitutively release endovanilloids

We quantified the concentration of AEA, NADA, OEA, PEA and the endocannabinoid arachidonoyl-glycerol (2-AG) in samples from mNPCs, fully-differentiated progeny from mNPCs and mouse HG-astrocytoma cells: mNPCs contained considerably high amounts of AEA, PEA and OEA; the endovanilloid levels in differentiated mNPCs or mouse HG-astrocytoma cells were much lower (Fig. 2a); NADA was not detectable in any sample (not shown). In mNPC-CM we found high concentrations of AEA (Fig. 2b), whereas culture supernatants from differentiated mNPCs or HG-astrocytoma cells contained much less AEA; other lipids were at the detection limit. Importantly, we observed that combined application of synthetic AEA, PEA and OEA exerts a cooperative effect on HG-astrocytoma cell death[22], which was blocked by I-RTX (Fig. 2c). Addition of fatty acid amide hydrolase (FAAH; which degrades ethanolamides[23]) fully abolished the cell death inducing effect of mNPC-CM (Fig. 2d) and of human NPC-CM (not shown).

The endocannabinoid 2-AG was detected in HG-astrocytoma cells at low levels, and was even less abundant in mNPCs (Fig. 2a) suggesting a role for endovanilloids (rather than endocannabinoids), as mediators of NPC-induced HG-astrocytoma cell death[22]. Consistently, addition of synthetic NADA to non-conditioned medium induced HG-astrocytoma cell death, whereas cannabinoid receptor blockade did not interfere with mNPC-CM induced cell death (Supplementary Figs. 2f, 2g, 3c and 3d). Next, we used FAAH-deficient mice ($Faah^{-/-}$), which have largely increased amounts of endocannabinoids/endovanilloids in the CNS[24], as a brain tumor model. Here, we investigated the effect of TRPV1 signaling on glioma growth (by implanting TRPV1-KD or control gliomas). We found that implantation of TRPV1 knock-down tumors resulted in much larger tumors compared to implantation of control tumors in $Faah^{-/-}$ animals (Fig. 2e). These data support our finding from *in vitro* experiments and show that even largely elevated levels of endogenous endocannabinoids/endovanilloids exert their tumor suppressive effects exclusively via TRPV1 receptors in our glioma model.

To assess the activity of NPC-released endovanilloids, we set-up a bioassay using dorsal root ganglion neurons (DRGs)[25] from wild-type and $Trpv1^{-/-}$ mice. DRGs were stimulated with mNPC-CM and responses were measured with Fura-2 based calcium-imaging. In wild-type mice, mNPC-CM induced Ca^{2+} responses in 5.4% of DRGs, which were also capsaicin sensitive, whereas only 0.85% responded to mNPC-CM alone. Interestingly, in $Trpv1^{-/-}$ mice, only 0.91% of DRGs responded to mNPC-CM, which would suggest that TRPV1 is required for the majority of the responses to mNPC-CM observed in wild-type mouse DRG

neurons (Supplementary Fig. 4a). Also, RT-PCR analysis of cultured mNPCs, their differentiated progeny and of whole brain extracts revealed that mNPCs express the major receptors and metabolic enzymes of the endo-vanilloid and -cannabinoid pathways (Supplementary Fig. 4b). These data support the view that AEA is a major constituent of mNPC-CM and that AEA is released from NPCs in physiologically relevant concentrations.

Furthermore, mNPC-CM stimulated TRPV1 mediated Ca^{2+} responses (single time-point ratiometric measurement of a bulk Ca^{2+} response in Fig. 2f; see also Supplementary Fig. 4c) in primary human glioblastoma cultures or human, rat and mouse HG-astrocytoma cell lines; capsaicin mediated Ca^{2+} signaling in mouse glioma cells (Supplementary Fig. 5a). We observed the ectopic expression of TRPV1 in the endoplasmic reticulum (ER; Supplementary Fig. 5b–e). The lower capsaicin-sensitivity of ER-located TRPV1 has been previously described[26], which may explain why a higher concentrations of capsaicin was required to induce cell death in HG-astrocytoma cells in previous studies[16].

Overall, we have shown that mNPCs constitutively synthesize and release endovanilloids, which induce Ca^{2+} responses and cell death in primary human glioblastomas and a range of HG-astrocytoma cell lines. Our data indicate that mouse and human NPCs use the same pathway for paracrine tumor suppression since addition of active FAAH or TRPV1 antagonists to NPC-CM of both species equally blocked HG-astrocytoma cell death.

TRPV1 induces cell death through ER stress

We investigated the gene expression pattern in mouse tumor cells after incubation with non-conditioned medium (controls) or mNPC-CM by microarrays (GSE37671). We found that ER stress genes like the activating transcription factor-3 (ATF3) were robustly upregulated in mNPC-CM treated mouse HG-astrocytoma cells, compared to controls. Immunocytochemical labeling and reporter gene assays in mNPC-CM treated GL261 cells showed that ATF3-expression is increased both in the cytoplasm and nucleus (versus controls) and regulates ATF3-responsive genes (Fig. 3a,b). Forced expression of ATF3 reduced the number of GL261 cells in culture and increased the number of $TUNEL^{+}$ tumor cells (Fig. 3c). Importantly, siRNA-mediated down-regulation of ATF3 expression (Supplementary Fig. 6a) in mouse HG-astrocytoma cells prevented mNPC-CM-induced tumor cell death (Fig. 3d). Hence, ATF3 is necessary and sufficient for mediating NPC-CM induced HG-astrocytoma cell death. The TRPV1 antagonist CZP blocked the mNPC-CM induced activation of the ATF3-dependent ER stress pathway in mouse HG-astrocytomas (Supplementary Fig. 6b,c).

Electron microscopy revealed that mNPC-CM treated GL261 cells had an enlarged ER as compared to controls (Fig. 4a; Supplementary Fig. 6d), which is a morphological hallmark of ER stress[27]. The effect of mNPC-CM (with or without CZP) on ER was quantified in primary human glioblastoma or human, rat and mouse HG-astrocytoma cell lines using ER-tracker (Fig. 4b,c). Likewise, the effect of human NPC-CM on ER-size in primary human glioblastomas was determined (Fig. 4d). In all HG-astrocytoma cells studied we detected a very robust increase in relative ER-size after stimulation with human or mouse NPC-CM, which was always attenuated by CZP (Fig. 4b–d; Supplementary Fig. 7). Additionally, we used synthetic AEA and ER stress inducers like tunicamycin or thapsigargin[28] at

concentrations that were sub-threshold for ER stress induction when applied alone. We found that the co-application of AEA plus tunicamycin or thapsigargin led to strong increases in relative ER-size in GL261 cells (Fig. 4e). Importantly, the combined substances had a clear cooperative effect on the rise in relative ER-size, confirming that vanilloid-induced signaling and ER stress are part of the same signal transduction pathway in HG-astrocytoma cells. In summary, these data show that human and mouse NPC-derived endovanilloids induce HG-astrocytoma cell death via the ER stress pathway (see cartoon in Fig. 4f).

Age-dependency of NPC-induced tumor suppression

To investigate if NPC-derived endovanilloids can suppress HG-astrocytomas *in vivo*, we performed orthotopic implantation of HG-astrocytomas into Nestin-GFP mice[8,9,17]. Inoculation of GL261 cells into young (30 day old) mice resulted in the association of many endogenous NPCs with the tumor[8,9,17] (Fig. 5a). Nestin-GFP^{+} NPCs accumulated at GL261 controls and TRPV1-KD tumors in equal density. Strikingly, we found that young mice injected with TRPV1-KD cells had significantly larger tumors, compared to controls (70% bigger; Fig. 5b). No difference in tumor size was detected in adult mice (90 days old; Fig. 5b). Furthermore, we used a previously established mouse model to investigate the anti-tumor effect of endogenous NPCs. We orthotopically implanted GL261 cells (control or TRPV1-KD) into cyclin-D2 knockout mice (*Ccnd2*$^{-/-}$, which have largely reduced adult neurogenesis[9,29]) or into their wild-type littermates. We found that tumor size in wild-type animals receiving HG-astrocytoma controls was at least 63% smaller as compared to wild-type mice receiving TRPV1-KD tumors cells or *Ccnd2*$^{-/-}$receiving either HG-astrocytoma controls or TRPV1-KD tumor cells (Fig. 5c). Next, we measured cell death *in vivo* by systemically delivering propidium-iodide (Fig. 5d)[30]. We noted that TRPV1-KD largely protected HG-astrocytoma cells from death.

In another set of experiments we tested the impact of NPC-released endovanilloids on the overall survival of a cohort of mice with HG-astrocytomas. Firstly, we orthotopically implanted GL261 cells (control or TRPV1-KD) into young mice and compared the cumulative survival. We observed that young wild-type tumor bearing mice (Fig. 5e) significantly outlived the older mice, unless the young mice were implanted with TRPV1-KD cells. These data show that younger mice have an intrinsic protective mechanism against HG-astrocytomas, which is dependent on endovanilloid signaling. In a second study we investigated if the survival promoting effect could be attributed specifically to NPCs. Therefore, we co-implanted adult mice with exogenously cultivated NPCs and HG-astrocytoma controls or TRPV1-KD tumor cells (Fig. 5f). We found that co-implantation of NPCs together with HG-astrocytoma controls in adult mice promoted survival, compared to injection of HG-astrocytoma control cells alone (compare Fig. 5e and 5f). Importantly, we also noticed that the survival promoting effect of NPCs in adult mice was absent after co-implantation with TRPV1-KD cells (Fig. 5f).

In summary, our study suggests that NPCs release endovanilloids *in vivo*, in a similar way as demonstrated for NPCs *in vitro*. Consistently, the extent of the NPC-mediated anti-tumor response depended on the level of adult neurogenesis.

Synthetic vanilloids as therapeutics for HG-astrocytomas

We investigated the therapeutic potential of a synthetic, non-pungent, blood-brain-barrier permeable vanilloid named Arvanil[31,32]. In organotypic brain slice cultures HG-astrocytomas were allowed to develop for 5 days. Addition of Temozolomide[33] (200 μM; the current standard of care for the treatment of glioblastoma patients) or Arvanil (50 nM) strongly reduced HG-astrocytoma size as compared to controls (Fig. 6a,b). Furthermore, Arvanil induced a TRPV1 dependent Ca^{2+} signal and TRPV1 dependent cell death in HG-astrocytomas (Supplementary Fig. 8). In further experiments we implanted TRPV1-KD or HG-astrocytoma controls and treated both groups with Arvanil as described above. We observed a significantly improved survival time in the control group compared to mice receiving TRPV1-KD tumor cells (Fig. 6c), suggesting that Arvanil elicits its therapeutic effect as a TRPV1 agonist. To determine if Arvanil would also increase survival in other HG-astrocytoma models, we implanted primary human glioblastoma cells (GBM1 and GBM2) into immune-compromised (*Scid*) mice. After one week, we examined tumor development and administered Arvanil[31] (a total of four i.p. injections with 1mg kg^{-1}) or vehicle. Strikingly, Arvanil-treatment robustly prolonged survival as compared to the vehicle-treated controls (Fig. 6d–f). Finally, we compared the effects of application of Arvanil and Temozolomide on survival after implantation of a third primary human HG-astrocytoma culture used in the present study (GBM3). We found that Arvanil prolonged survival in a cohort of immune-deficient mice that received HG-astrocytoma cells that did not respond to Temozolomide (given[34] once daily for 5 days at 100 mg kg^{-1}; Fig. 6f). These data show the potential clinical value of an experimental HG-astrocytoma therapy using vanilloids, which may also offer a new therapeutic option for Temozolomide resistant HG-astrocytomas[35].

Discussion

We have shown that HG-astrocytomas express high levels of TRPV1 and that TRPV1 stimulation induces tumor cell death. Neural stem and precursor cells home in on HG-astrocytomas and release anti-tumorigenic TRPV1 agonists (i.e. fatty acid ethanolamides). Endogenous and exogenous NPCs show extensive tropism for brain tumors[6–10]. However, the number of endogenous NPCs accumulating at HG-astrocytomas depends on the proliferative activity in the stem cell niche and declines before the onset of adulthood[9]. Hence, the recruitment of large numbers of NPCs to a tumor, and concomitantly the anti-tumorigenic release of endovanilloids, is restricted to the young brain. Additionally, other age-related changes in neural stem cell physiology may also impinge on the capacity for NPC-mediated tumor suppression[36,37].

We demonstrated that NPCs are a primary source of endogenous TRPV1 and cannabinoid receptor agonists like AEA[15,38]. This is substantiated by the detection of high amounts of AEA and related acyl-ethanolamides in undifferentiated NPCs, by the finding that NPC-released factors evoke TRPV1 dependent Ca^{2+} responses in DRGs and HG-astrocytomas, that the tumor suppressive effect of NPC-CM is lost after addition of FAAH and that NPC-induced HG-astrocytoma cell death is TRPV1 dependent *in vitro* and *in vivo*. These data are

in agreement with previous reports indicating that synthetic AEA induces HG-astrocytoma cell death[39].

A role for TRP-channels in tumor suppression was previously suggested by us and others[40–44], but the present study is the first to identify NPCs as a cellular source for tumor suppressive endovanilloids and to uncover the role of NPC-released TRPV1-agonists and -modulators on HG-astrocytoma cell death. Overall, our study suggests that endovanilloids are intrinsic tumor suppressors in the brain and that synthetic vanilloid compounds may have clinical potential for brain tumor treatment.

Materials and Methods

Animals

Animal experiments were carried out in compliance with the German laws on animal welfare, and the animal protocols were approved by the Landesamt für Gesundheit und Soziales (LaGeSo) in Berlin. Wild type C57BL/6 mice, Nestin-GFP [18] mice, *Trpv1*$^{-/-}$mice [45], *Ccnd2*$^{-/-}$ [29], *Faah*$^{-/-}$ [24] and *Scid* mice (B6.CB17-*Prkdc*^{scid}/SzJ; Charles River Breeding Laboratories; Schöneiche, Germany) were housed with a 12 h light/dark cycle and received food ad libitum.

SVZ specimen, tumor specimen, glioblastoma cDNA-arrays and normal brain cDNA-arrays

Normal SVZ specimens were obtained as part of planned resections during anterior temporal lobectomy for the treatment of intractable epilepsy from mesial temporal sclerosis. We obtained the ethical approval (given by the ethics committee of Charité university clinics; license numbers EA112/2001, EA3/023/06 and EA2/101/08. Tumor samples were obtained from (otherwise untreated) primary glioblastomas, according to governmental and internal (Charité) rules and regulations; cDNA samples and tissue arrays from human brain tumors and from tumor-free brain were obtained from OriGene.

Cell culture

All glioblastoma cells were maintained as described for neurospheres[46]. Mouse, rat, human HG-astrocytoma cell lines and 293T cells were obtained from the National Cancer Institute, NCI-Frederick and from ATCC. Mouse NPCs were gained from SVZ; dorsal root ganglia (DRG) neurons were prepared from both wild-type and *Trpv1*$^{-/-}$ adult mice as described previously[25].

shRNA experiments

The pLKO.1 shRNA vector was from BioCat. The validity of the shRNA mediated knockdown was affirmed on the protein level, by Western-blotting and FACS analysis, as described[47] and on the functional level. The TRPV1 rescue construct was mutated in the seed-region of the shRNA knock-down construct[21].

Cytotoxicity assay

CytoTox-Fluor™ cytotoxicity assays (Promega) were measured (485nm/520nm) with the fluorometer (TECAN).

TUNEL assay

TUNEL$^+$ cells were quantified using the DELFIA cell-based fragmentation assay (PerkinElmer).

Microarray analysis

cDNA microarrays[48] were generated using ~20,000 murine cDNA clones (arrayTAG clone collection) from LION Bioscience, six arrays were used in total. Image acquisition and data analysis was done as described[48].

HPLC and Mass-spectrometry

Lipids were purified by open-bed chromatography on silica gel and AEA, 2 AG, PEA, OEA and NADA were analyzed by isotope dilution-liquid chromatography/atmospheric pressure chemical ionization/mass spectrometry[49–51].

Peptides for the development of a SRM method (selected reaction monitoring) were selected. Cells were lysed, protease digested, purified, separated by HPLC and electrosprayed into the mass spectrometer (ABSciex Q-TRAP 4000). For the data analysis the MultiQuant (ABSciex) and the R-software packages (www.R-project.org) were used[52].

Calcium measurements

Cells were loaded with Fura-2 acetoxymethyl ester (TEF-Lab), excited at 340 and 380 nm and imaged with a 510 nm long-pass filter; the results are presented as the ratio between the emission signals acquired using the two excitation wavelengths.

Real-time PCR

qRT-PCR was performed on the iCycler IQ 5 multicolor real-time detection system (Bio-Rad), using absolute SYBR green fluorescein (ABgene). Oligonucleotides were purchased from Invitrogen.

Western blot

Membranes were incubated with specific antibodies and Western blots were developed using the chemiluminescence method (GE-Healthcare).

Tumor implantation

Surgical procedures were performed as described[8,9]: Anaesthetized mice received (2×10^4 G261 cells/1μl) alone or in combination with exogenously cultivated NPCs (6×10^4 precursor cells.

Immunofluorescence and Microscopy

All stainings and microscopy for NPC- and HG-astrocytomas markers was carried out as described previously[53].

Electron microscopy

For ER- visualization, ultrathin cryosections (70 nm) of fixed HG-astrocytoma cells were contrasted, stabilized[54] and examined with a Zeiss 910 electron microscope. For preembedding immunogold labeling, HG-astrocytoma cells were fixed in 4% paraformaldehyde and 1% glutaraldehyde and incubated with TRPV1 antibody.

Cell counting and unbiased stereology

In every 12th axial section we sampled the area that was primarily infiltrated by the tumor in an unbiased approach using the optical fractionator procedure (StereoInvestigator, MicroBrightField Inc.). Tumor volume was quantified according to the Cavalieri principle.

Statistical analysis

Survival statistics were analyzed using MatLab software (Natick). Bar diagrams are shown as mean values ± standard deviation of the mean. Comparisons among the groups were performed with the Student's *t* test, Fishers exact test and the Wilcoxon rank test (as indicated).

Supplementary Material

Refer to Web version on PubMed Central for supplementary material.

Acknowledgments

We thank G. Gargiulo, O. Daumke, and J. Kurreck for discussion of the manuscript, S. Kitajima for ATF3 constructs, L. Kaczmarek and M. Szymanska for help with the *Ccnd2*$^{-/-}$ mice. Funding by Helios-Clinics (HeFoFö-ID1148) and by US National Institute of Health (DA-009789 to VDM) is gratefully acknowledged.

References

1. Sanai N, Alvarez-Buylla A, Berger MS. Neural stem cells and the origin of gliomas. The New England journal of medicine. 2005; 353:811–822. [PubMed: 16120861]
2. Ohgaki H, Kleihues P. Epidemiology and etiology of gliomas. Acta neuropathologica. 2005; 109:93–108. [PubMed: 15685439]
3. Ohgaki H, Kleihues P. Genetic pathways to primary and secondary glioblastoma. Am J Pathol. 2007; 170:1445–1453. [PubMed: 17456751]
4. Knoth R, et al. Murine features of neurogenesis in the human hippocampus across the lifespan from 0 to 100 years. PloS one. 5:e8809. [PubMed: 20126454]
5. Leuner B, Kozorovitskiy Y, Gross CG, Gould E. Diminished adult neurogenesis in the marmoset brain precedes old age. Proceedings of the National Academy of Sciences of the United States of America. 2007; 104:17169–17173. [PubMed: 17940008]
6. Assanah M, et al. Glial progenitors in adult white matter are driven to form malignant gliomas by platelet-derived growth factor-expressing retroviruses. The Journal of neuroscience: the official journal of the Society for Neuroscience. 2006; 26:6781–6790. [PubMed: 16793885]
7. Assanah MC, et al. PDGF stimulates the massive expansion of glial progenitors in the neonatal forebrain. Glia. 2009
8. Glass R, et al. Glioblastoma-induced attraction of endogenous neural precursor cells is associated with improved survival. The Journal of neuroscience: the official journal of the Society for Neuroscience. 2005; 25:2637–2646. [PubMed: 15758174]
9. Walzlein JH, et al. The antitumorigenic response of neural precursors depends on subventricular proliferation and age. Stem Cells. 2008; 26:2945–2954. [PubMed: 18757298]

10. Aboody KS, et al. Neural stem cells display extensive tropism for pathology in adult brain: evidence from intracranial gliomas. Proceedings of the National Academy of Sciences of the United States of America. 2000; 97:12846–12851. [PubMed: 11070094]
11. Suzuki T, et al. Inhibition of glioma cell proliferation by neural stem cell factor. J Neurooncol. 2005; 74:233–239. [PubMed: 16187020]
12. Staflin K, et al. Neural progenitor cell lines inhibit rat tumor growth in vivo. Cancer research. 2004; 64:5347–5354. [PubMed: 15289341]
13. Staflin K, Zuchner T, Honeth G, Darabi A, Lundberg C. Identification of proteins involved in neural progenitor cell targeting of gliomas. BMC Cancer. 2009; 9:206. [PubMed: 19558675]
14. Starowicz K, Nigam S, Di Marzo V. Biochemistry and pharmacology of endovanilloids. Pharmacol Ther. 2007; 114:13–33. [PubMed: 17349697]
15. Toth A, Blumberg PM, Boczan J. Anandamide and the vanilloid receptor (TRPV1). Vitam Horm. 2009; 81:389–419. [PubMed: 19647120]
16. Szallasi A, Cortright DN, Blum CA, Eid SR. The vanilloid receptor TRPV1: 10 years from channel cloning to antagonist proof-of-concept. Nat Rev Drug Discov. 2007; 6:357–372. [PubMed: 17464295]
17. Chirasani SR, et al. Bone morphogenetic protein-7 release from endogenous neural precursor cells suppresses the tumourigenicity of stem-like glioblastoma cells. Brain. 2010; 133:1961–1972. [PubMed: 20513660]
18. Yamaguchi M, Saito H, Suzuki M, Mori K. Visualization of neurogenesis in the central nervous system using nestin promoter-GFP transgenic mice. Neuroreport. 2000; 11:1991–1996. [PubMed: 10884058]
19. Zhao C, Deng W, Gage FH. Mechanisms and functional implications of adult neurogenesis. Cell. 2008; 132:645–660. [PubMed: 18295581]
20. Okano H, Imai T, Okabe M. Musashi: a translational regulator of cell fate. J Cell Sci. 2002; 115:1355–1359. [PubMed: 11896183]
21. Cullen BR. Enhancing and confirming the specificity of RNAi experiments. Nat Methods. 2006; 3:677–681. [PubMed: 16929311]
22. Lambert DM, Di Marzo V. The palmitoylethanolamide and oleamide enigmas: are these two fatty acid amides cannabimimetic? Curr Med Chem. 1999; 6:757–773. [PubMed: 10469890]
23. Ueda N, Puffenbarger RA, Yamamoto S, Deutsch DG. The fatty acid amide hydrolase (FAAH). Chem Phys Lipids. 2000; 108:107–121. [PubMed: 11106785]
24. Cravatt BF, et al. Supersensitivity to anandamide and enhanced endogenous cannabinoid signaling in mice lacking fatty acid amide hydrolase. Proceedings of the National Academy of Sciences of the United States of America. 2001; 98:9371–9376. [PubMed: 11470906]
25. Sturzebecher AS, et al. An in vivo tethered toxin approach for the cell-autonomous inactivation of voltage-gated sodium channel currents in nociceptors. J Physiol. 2010; 588:1695–1707. [PubMed: 20308253]
26. Gallego-Sandin S, Rodriguez-Garcia A, Alonso MT, Garcia-Sancho J. The endoplasmic reticulum of dorsal root ganglion neurons contains functional TRPV1 channels. J Biol Chem. 2009; 284:32591–32601. [PubMed: 19778904]
27. Hori O, et al. Role of Herp in the endoplasmic reticulum stress response. Genes Cells. 2004; 9:457–469. [PubMed: 15147274]
28. Xu C, Bailly-Maitre B, Reed JC. Endoplasmic reticulum stress: cell life and death decisions. J Clin Invest. 2005; 115:2656–2664. [PubMed: 16200199]
29. Kowalczyk A, et al. The critical role of cyclin D2 in adult neurogenesis. J Cell Biol. 2004; 167:209–213. [PubMed: 15504908]
30. Cevik IU, Dalkara T. Intravenously administered propidium iodide labels necrotic cells in the intact mouse brain after injury. Cell Death and Differentiation. 2003; 10:928–929. [PubMed: 12868000]
31. Melck D, Bisogno T, De Petrocellis L, Chuang H, Julius D, Bifulco M, Di Marzo V. Unsaturated long-chain N-acyl-vanillyl-amides (N-AVAMs): vanilloid receptor ligands that inhibit anandamide-facilitated transport and bind to CB1 cannabinoid receptors. Biochem Biophys Res Commun. 1999 Aug 19; 262(1):275–84. [PubMed: 10448105]

32. Veldhuis WB, et al. Neuroprotection by the endogenous cannabinoid anandamide and arvanil against in vivo excitotoxicity in the rat: role of vanilloid receptors and lipoxygenases. The Journal of neuroscience: the official journal of the Society for Neuroscience. 2003; 23:4127–4133. [PubMed: 12764100]
33. Fisher T, et al. Mechanisms operative in the antitumor activity of temozolomide in glioblastoma multiforme. Cancer J. 2007; 13:335–344. [PubMed: 17921733]
34. McConville P, et al. Magnetic resonance imaging determination of tumor grade and early response to temozolomide in a genetically engineered mouse model of glioma. Clinical cancer research: an official journal of the American Association for Cancer Research. 2007; 13:2897–2904. [PubMed: 17504989]
35. Mrugala MM, Chamberlain MC. Mechanisms of disease: temozolomide and glioblastoma--look to the future. Nat Clin Pract Oncol. 2008; 5:476–486. [PubMed: 18542116]
36. Conover JC, Shook BA. Aging of the Subventricular Zone Neural Stem Cell Niche. Aging and disease. 2011; 2:149–163. [PubMed: 22140636]
37. Khan MA, Lie DC. MicroRNA - a contributor to age-associated neural stem cell dysfunction? Aging. 2011; 3:182–183. [PubMed: 21415460]
38. Di Marzo V, Gobbi G, Szallasi A. Brain TRPV1: a depressing TR(i)P down memory lane? Trends Pharmacol Sci. 2008; 29:594–600. [PubMed: 18947889]
39. Maccarrone M, Lorenzon T, Bari M, Melino G, Finazzi-Agro A. Anandamide induces apoptosis in human cells via vanilloid receptors. Evidence for a protective role of cannabinoid receptors. J Biol Chem. 2000; 275:31938–31945. [PubMed: 10913156]
40. Izzo AA, et al. Increased endocannabinoid levels reduce the development of precancerous lesions in the mouse colon. J Mol Med. 2008; 86:89–98. [PubMed: 17823781]
41. Prevarskaya N, Zhang L, Barritt G. TRP channels in cancer. Biochim Biophys Acta. 2007; 1772:937–946. [PubMed: 17616360]
42. Bode AM, et al. Transient receptor potential type vanilloid 1 suppresses skin carcinogenesis. Cancer research. 2009; 69:905–913. [PubMed: 19155296]
43. Visnyei K, et al. A molecular screening approach to identify and characterize inhibitors of glioblastoma stem cells. Molecular cancer therapeutics. 2011; 10:1818–1828. [PubMed: 21859839]
44. Beatrice Morelli M, et al. The Transient Receptor Potential Vanilloid-2 (TRPV2) cation channel impairs glioblastoma stem-like cell proliferation and promotes differentiation. International journal of cancer. Journal international du cancer. 201210.1002/ijc.27588
45. Caterina MJ, et al. Impaired nociception and pain sensation in mice lacking the capsaicin receptor. Science. 2000; 288:306–313. [PubMed: 10764638]
46. Lee J, et al. Tumor stem cells derived from glioblastomas cultured in bFGF and EGF more closely mirror the phenotype and genotype of primary tumors than do serum-cultured cell lines. Cancer Cell. 2006; 9:391–403. [PubMed: 16697959]
47. Grunweller A, et al. Comparison of different antisense strategies in mammalian cells using locked nucleic acids, 2′-O-methyl RNA, phosphorothioates and small interfering RNA. Nucleic Acids Res. 2003; 31:3185–3193. [PubMed: 12799446]
48. Gurok U, et al. Gene expression changes in the course of neural progenitor cell differentiation. The Journal of neuroscience: the official journal of the Society for Neuroscience. 2004; 24:5982–6002. [PubMed: 15229246]
49. Devane WA, et al. Isolation and structure of a brain constituent that binds to the cannabinoid receptor. Science. 1992; 258:1946–1949. [PubMed: 1470919]
50. Bisogno T, Maurelli S, Melck D, De Petrocellis L, Di Marzo V. Biosynthesis, uptake, and degradation of anandamide and palmitoylethanolamide in leukocytes. J Biol Chem. 1997; 272:3315–3323. [PubMed: 9013571]
51. Marsicano G, et al. The endogenous cannabinoid system controls extinction of aversive memories. Nature. 2002; 418:530–534. [PubMed: 12152079]
52. de Godoy LM, et al. Comprehensive mass-spectrometry-based proteome quantification of haploid versus diploid yeast. Nature. 2008; 455:1251–1254. [PubMed: 18820680]

53. Kempermann G, Gast D, Kronenberg G, Yamaguchi M, Gage FH. Early determination and long-term persistence of adult-generated new neurons in the hippocampus of mice. Development. 2003; 130:391–399. [PubMed: 12466205]

54. Reimer TA, et al. Reevaluation of the 22-1-1 antibody and its putative antigen, EBAG9/RCAS1, as a tumor marker. BMC Cancer. 2005; 5:47. [PubMed: 15904507]

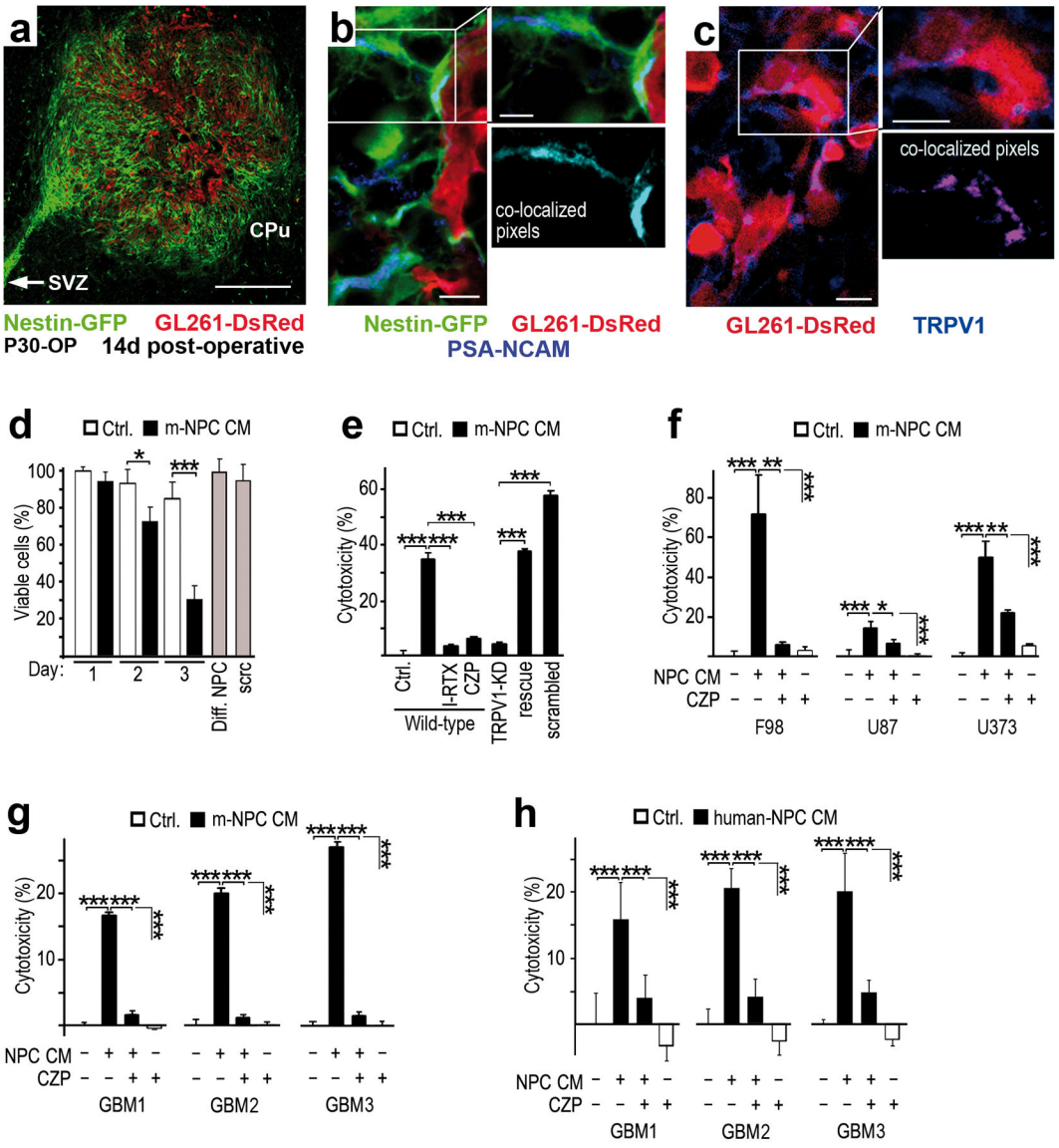

Figure 1. NPC-released TRPV1 agonists induce HG-astrocytoma cell death

(**a**) After 14 days of tumor development large numbers of Nestin-GFP$^+$ cells were observed at a DsRed$^+$ glioma in the caudate putamen (CPu) of young mice (postnatal day 30 operated; P30-OP; n = 12, male and female for all immunohistochemistry); arrow indicates subventricular zone (SVZ). (**b**) Glioma-associated Nestin-GFP$^+$ cells express PSA-Ncam (blue); a single cell (boxed area) is magnified, colocalizing pixels of a single optical section are shown. (**c**) Glioma cells are immunopositive for TRPV1 (blue); a single cell (boxed area) is magnified, colocalizing pixels of a single optical section are shown. (**d**) Viability of mouse GL261 glioma cells is reduced after stimulation with mouse NPC-conditioned medium (mNPC-CM), but not with non-conditioned medium (Ctrl) or other control media (grey bars). (**e**) mNPC-CM induced cytotoxicity of GL261cells was blocked by CZP and TRPV1 knock-down (TRPV1-KD), but not control-shRNA (scrambled); rescue of the TRPV1-KD fully restores the effect of mNPC-CM. (**f–h**) Relative cytotoxicity of primary

human glioblastoma cells (**g, h**) and HG-astrocytoma cell lines (**f**) after incubation with mNPC-CM (**f**, **g**) or human NPC-CM (**h**) with or without CZP. Scale bar represents: 500 μm in (a); 10 μm in (b), 6 μm for the magnified cell in (b); 10 μm in (c); 10 μm for the magnified cell in (c). Statistical significance (*t*-test) is indicated: *** for $p < 0.001$; ** for $p < 0.005$; * for $p < 0.05$.

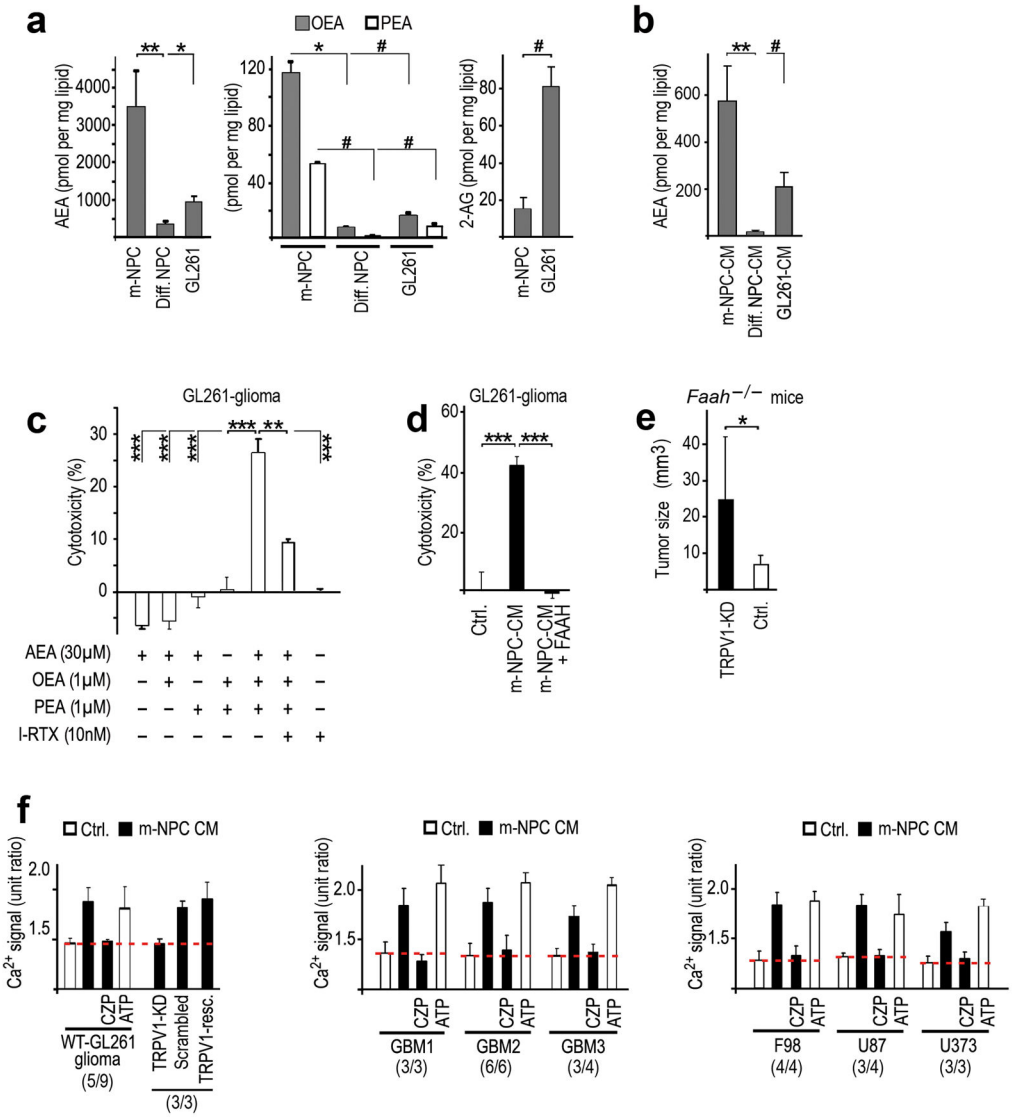

Figure 2. NPC-released fatty acid ethanolamides induce cell death in HG-astrocytomas

(**a**) Quantification of AEA, OEA, PEA and 2-AG in mNPCs, differentiated (Diff.) NPC and GL261 HG-astrocytomas. (**b**) Quantification of AEA in conditioned medium from mNPCs, Diff. NPC and GL261 cells. (**c**) HG-astrocytoma cell death is cooperatively induced after co-application of AEA, PEA and OEA, but not by a sub-threshold concentration of AEA alone; I-RTX blunted AEA + PEA + OEA induced HG-astrocytoma cell death. (**d**) Cytotoxicity of GL261 cells exposed to non-conditioned medium (Ctrl.), mNPC-CM or mNPC-CM plus fatty acid amide hydrolase (FAAH). (**e**) Glioma growth in *Faah*$^{-/-}$ mice with control (Ctrl.) or TRPV1-KD tumors ($n \geq 7$ per experimental group, male and female). (**f**) Ca^{2+} responses in wild-type, TRPV1 knock-down (TRPV1-KD) and TRPV1 rescue GL261 cells, stimulated with mNPC-CM; Ca^{2+} responses to NPC-CM were also recorded from three different primary human glioblastoma cultures (GBM, central panel) and HG-astrocytoma cell lines, (right panel); CZP blocked the NPC-CM evoked Ca^{2+} signals in all cases; dotted red line indicates baseline values for each experiment; ATP (1 mM) induced a

Ca^{2+} response in all experiments, indicating that all cells were alive and responsive. Statistical significance is indicated; Fishers exact test in (a) and (b); *t* test (c) through (e): *** for $p < 0.001$, ** for $p < 0.005$, * for $p < 0.05$; Wilcoxon rank test: # for $p < 0.001$.

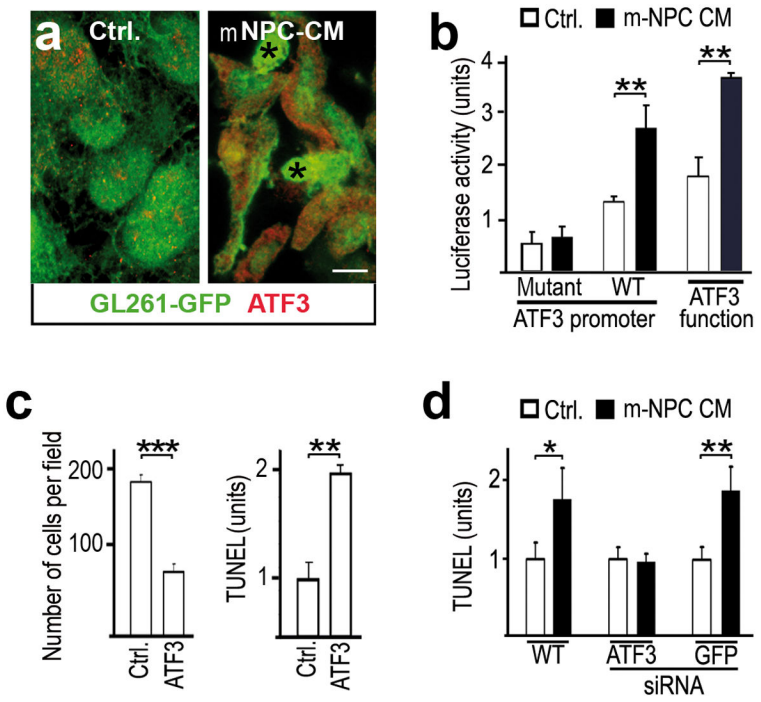

Figure 3. NPC-released TRPV1 agonists trigger the ATF3 pathway in HG-astrocytomas

(**a**) ATF3 expression in HG-astrocytomas (GL261 cells expressing GFP) exposed to non-conditioned medium (Ctrl.) or mNPC-CM. (**b**) The ATF3-gene promoter is induced in GL261 cells after stimulation with mNPC-CM; a gene promoter with an ATF3 binding site (ATF3 function) is also induced after stimulation with mNPC-CM. (**c**) Over-expression of ATF3 reduced GL261 cell density and induced DNA-fragmentation (TUNEL). (**d**) siRNA for ATF3 prevents NPC-CM induced nuclear strand breaks in GL261 HG-astrocytoma cells. Scale bar represents: 10 μm in (a). Statistical significance is indicated (*t* test): *** for $p < 0.001$, ** for $p < 0.005$, * for $p < 0.05$.

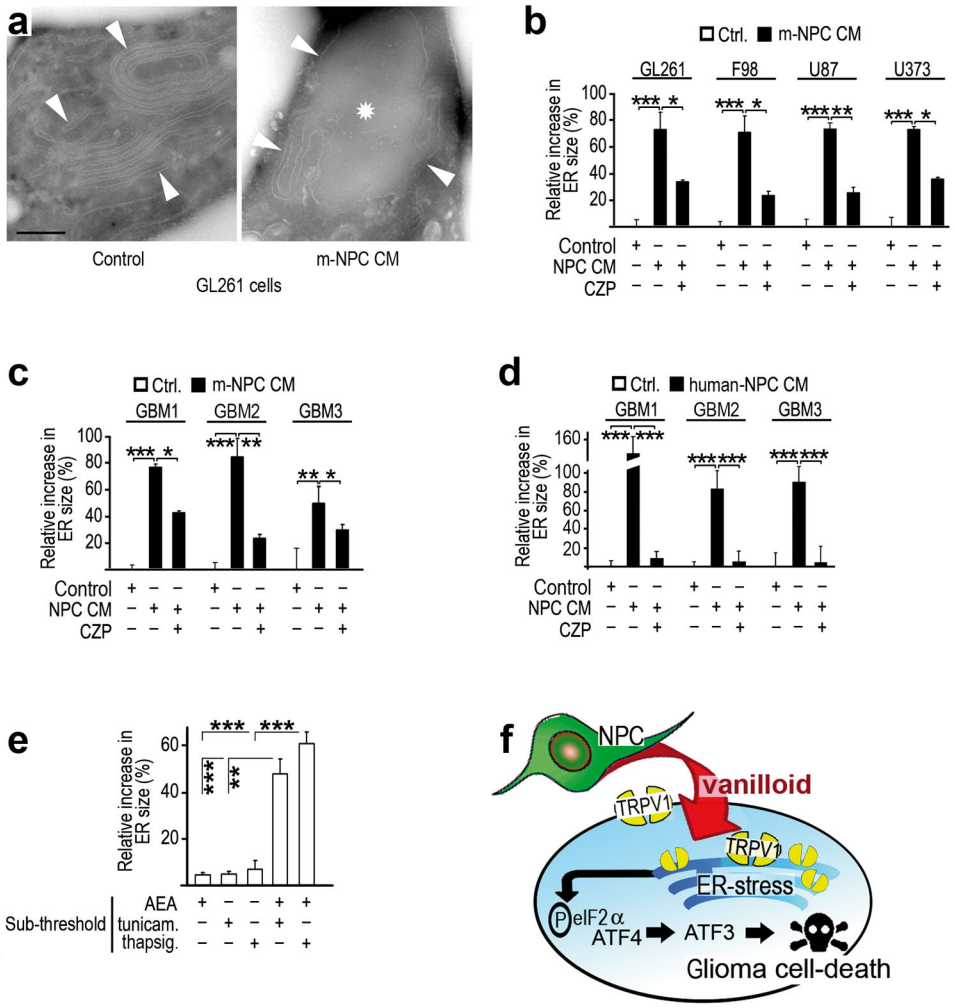

Figure 4. NPC-released TRPV1 agonists induce ER stress mediated cell death

(**a**) Ultrastructure of GL261 HG-astrocytoma cells after incubation with mNPC-CM or control medium; ER-membrane is highlighted by arrowheads, inflated ER lumen is indicated by an asterisk. (**b**) The relative increase in ER-size after incubation with mNPC-CM was quantified in various HG-astrocytoma cell lines. (**c**) ER-size was quantified in primary human glioblastoma cells after incubation with mNPC-CM and human NPC-CM (**d**). (**e**) Vanilloids and pharmacological ER stress inducers have cooperative effects: sub-threshold concentrations of the combined substances induce ER-enlargement. (**f**) Cartoon illustrating that NPCs constitutively release endovanilloids (fatty acid ethanolamides like AEA, PEA and OEA), which traverse the plasma-membrane of HG-astrocytomas and stimulate TRPV1 by docking to an intracellular receptor binding-site. NPC-induced TRPV1 activation (preponderantly located in the ER; see Supplementary Fig. 5) triggers the ATF3-dependent ER stress pathway in HG-astrocytomas, which includes activation of eiF2α and ATF4[28] (see Supplementary Fig. 6). Increased expression of ATF3 is necessary and sufficient to mediate HG-astrocytoma cell death. Scale bar represents: 500 nm in (a). Statistical significance (*t* test) is indicated: *** for $p < 0.001$; ** for $p < 0.005$; * for $p < 0.05$.

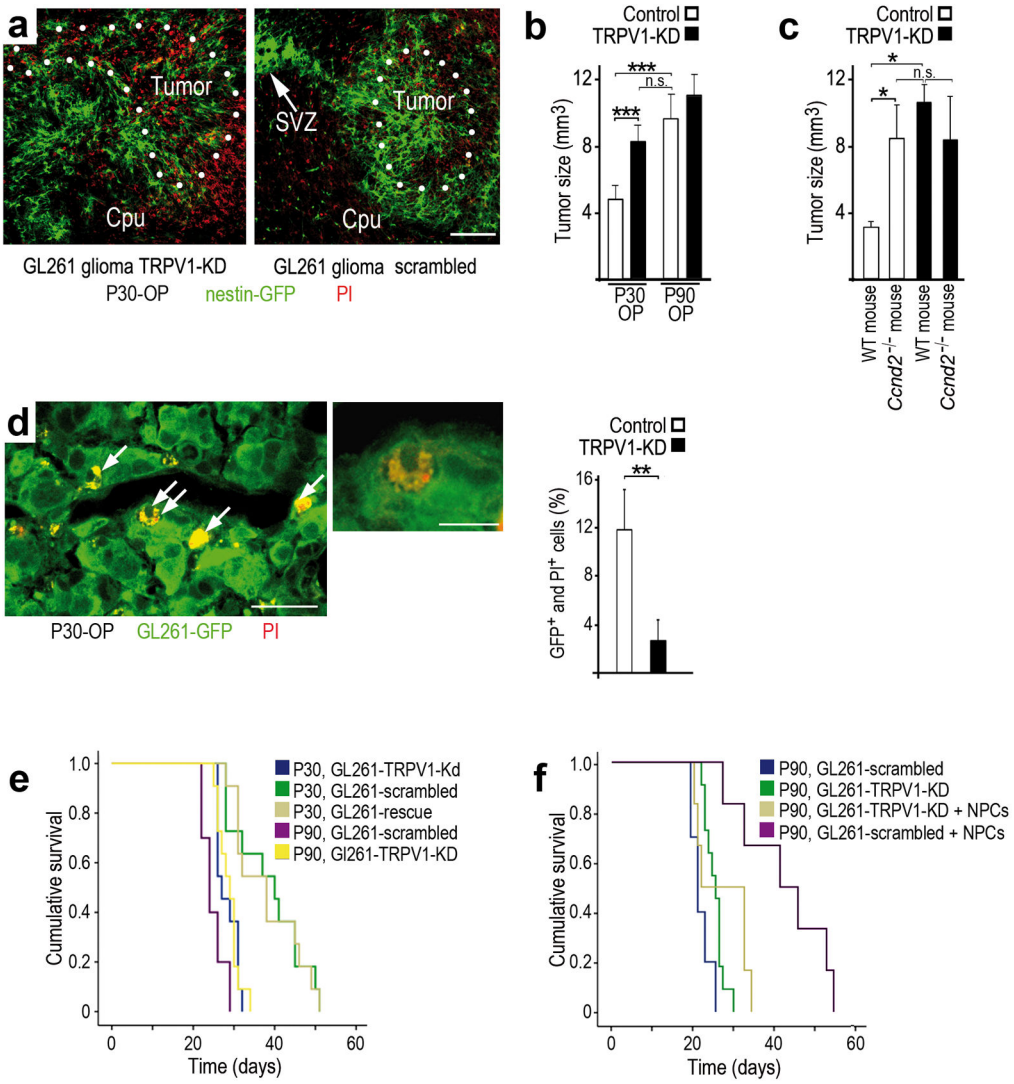

Figure 5. NPC-mediated tumor suppression by endovanilloids is restricted to the young brain

(**a**) GL261-TRPV1-KD cells induce larger tumors than controls (scrambled) within the caudate putamen (CPu) of Nestin-GFP mice at P30 (n=14, male and female); propidium iodide labeling (PI, red) indicates dying parenchymal cells. (**b**) Tumor size of TRPV1-KD and control HG-astrocytomas in P30-OP and P90-OP animals (n = 6 per experimental group, male and female). (**c**) Tumor size of TRPV1-KD and control HG-astrocytomas in P30-OP wild-type (WT) or *Ccnd2*$^{-/-}$ mice, which have reduced neurogenesis (*n* = 4 mice per experimental group, male and female). (**d**) Nuclear PI-labeling indicates dying GL261-GFP cells (arrows), a single PI^{+} tumor cell is magnified (double-arrows); Quantification of PI-labeled (dying) tumor cells: TRPV1-KD reduced HG-astrocytoma cell death, compared to wild-type tumors (*n* = 14 mice, male and female). (**e, f**) The proportion of mice (P30 or P90) surviving HG-astrocytomas, i.e. inoculation with control (scrambled or rescue) or TRPV1-KD GL261 cells; (**e**) note that P30-OP mice outlive P90-OP mice, unless given TRPV1-KD tumor cells (*n* ≥ 10 mice per group; male and female); (**f**) note that co-implantation of P90-OP mice with NPCs and control HG-astrocytomas (scrambled), but not

with TRPV1-KD tumors, improves survival ($n \geq 6$ mice per group; male and female). Scale bar represents: 300 μm in (a); 30 μm in (d, left) 10 μm in (d, right). Statistical significance (*t* test) is indicated: *** for $p < 0.001$; ** for $p < 0.005$; * for $p < 0.05$. Survival is statistically different with: $p < 0.001$ (in e and f).

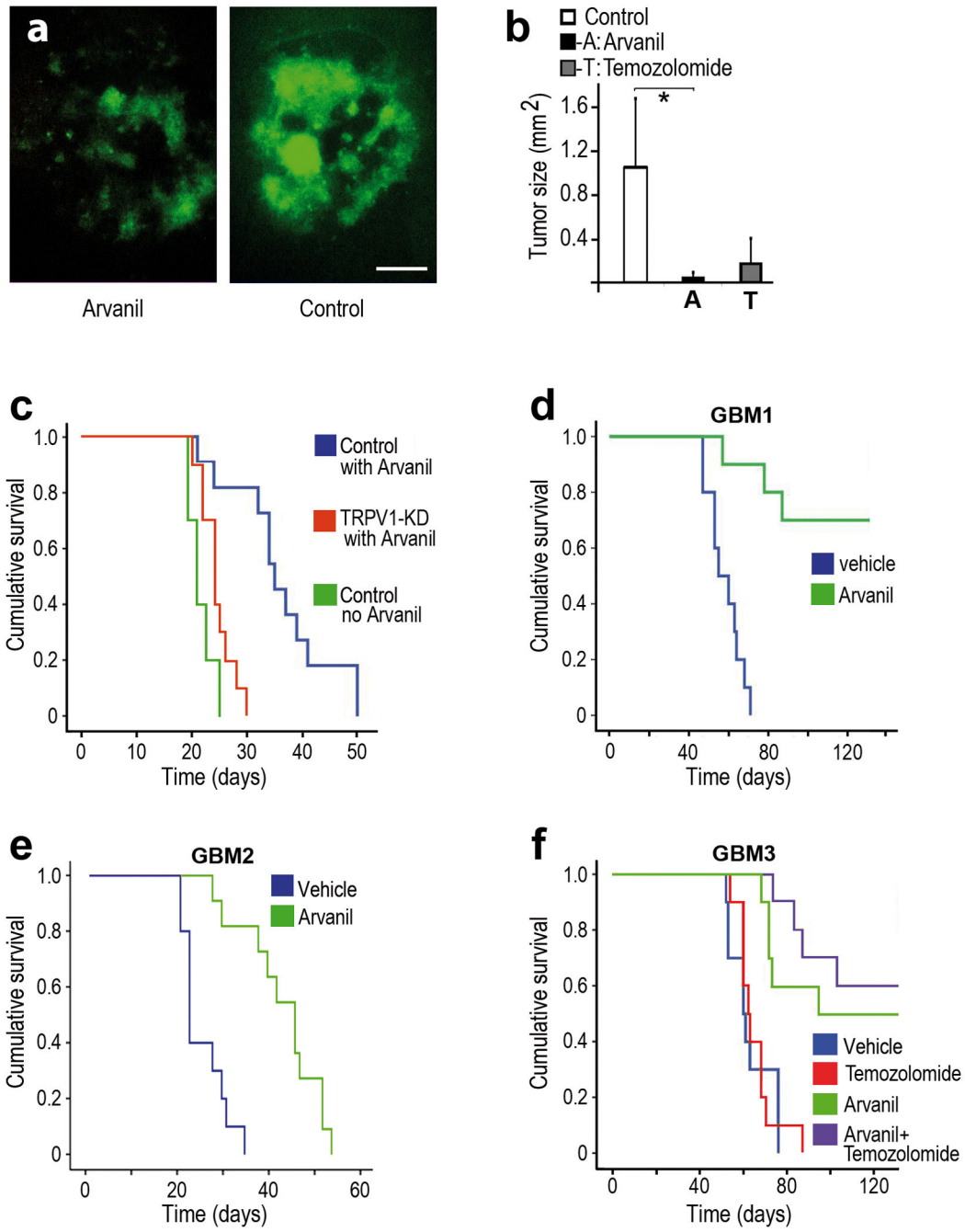

Figure 6. The synthetic vanilloid Arvanil has therapeutic effects on experimental HG-astrocytomas

(**a**) Tumor size of GFP$^+$ GL261 cells in brain slice cultures is reduced after treatment with 50 nM Arvanil compared to untreated controls; (**b**) Tumors sizes from brain slice experiments with Arvanil-treated (A) or Temozolomide-treated (T) HG-astrocytomas. (**c**) The proportion of mice surviving orthotopic HG-astrocytomas (control or TRPV1-KD GL261 cells) after receiving four i.p. injections of Arvanil or vehicle; note that Arvanil significantly improved survival only in animals receiving control HG-astrocytoma cells ($n \geq$

10 mice per group; male and female). (**d, e**) The proportion of immune-deficient mice surviving orthotopic human primary glioblastomas (GBM1 or GBM2); note that Arvanil treatment of established tumors significantly improved survival ($n \geq 10$ mice per group; all female). (**f**) The proportion of immune-deficient mice surviving orthotopic human primary glioblastoma (GBM3); note that Arvanil treatment of established tumors (alone or together with Temozolomide) significantly improved survival (n ≥ 10 mice per group; all female). Scale bar represents: 300 μm in (a); Statistical significance (*t* test) is indicated: * for $p < 0.05$. Survival is statistically different with: $p < 0.001$.